Corrosion-Induced Degradation of Reinforced Concrete Elements: Preliminary Results, in: Service Life and Durability of Reinforced Concrete Structures

Olfa Loukil, Lucas Adelaide, Véronique Bouteiller, Thierry Chaussadent, Frédéric Ragueneau, Xavier Bourbon, Laurent Trenty

CORROSION-INDUCED DEGRADATION OF REINFORCED CONCRETE ELEMENTS: PRELIMINARY RESULTS

O. LOUKIL [(1)], L. ADELAIDE [(1)], V. BOUTEILLER [(1)], M. QUIERTANT [(2)], T. CHAUSSADENT [(3)], F.RAGUENEAU[(4)], X. BOURBON[(5)], L. TRENTY[(5)]

[(1)]*Université Paris-Est, MAST, SDOA, IFSTTAR, F-77447 Marne-la-Vallée, France.*
[(2)]*Université Paris-Est, MAST, EMMS, IFSTTAR, F-77447 Marne-la-Vallée, France.*
[(3)]*Université Paris-Est, MAST, CPDM, IFSTTAR, F-77447 Marne-la-Vallée, France.*
[(4)]*LMT/ENS Cachan/CNRS/Univ. Paris 6/PRES UniverSud, 94230 Cachan, France.*
[(5)]*Andra, F-92298 Châtenay-Malabry cedex, France.*

Abstract

Steel reinforcement corrosion is the predominant cause of deterioration of reinforced concrete structures. Corrosion products can induce concrete cracking, loss of adhesion at the steel-concrete interface, loss of reinforcing bar cross-section, and even spalling of the concrete cover.

This study investigates the durability problems related to corrosion of the reinforcement by combining experimental and numerical approaches. This paper particularly focuses on the experimental methodology used for the evaluation of the development over time of damages (steel corrosion products formation and crack patterns) induced by accelerated corrosion tests. The accelerated corrosion tests were carried out by applying a constant current between a reinforcement bar used as an anode and an external counter electrode. The corrosion process was monitored by measuring relevant electrochemical parameters, i.e. free corrosion potential, polarization resistance and electrical concrete resistance. The aim of this paper is to characterize the crack pattern (orientation, length and width) and the corrosion products layers according to the current density and the time.

Keywords: reinforced concrete, corrosion, rust layer, cracks, electrochemistry

1 Introduction

Steel reinforcement corrosion in Reinforced Concrete (RC) structures of is a major issue of concern for asset owners. The consequences of this phenomenon are degradation of the steel/concrete bond, reduction of the steel reinforcing bar (rebar) cross-section, and concrete cover cracking [1]. This last aspect results from the production of oxides which occupy a volume that is two to seven times higher than the parent steel. Actually, when this production is greater than diffusion of iron oxide into the concrete pores, pressure increases at the interface between the rebar and the surrounding concrete [2], [3], [4], [5] and exerts tensile stresses in the concrete all along the corroding reinforcements. If these stresses exceed the concrete tensile strength, cracking initiates and propagates towards the outer surface leading to the delamination of the concrete cover [6] [7]. Due to the deleterious mechanical effect of the corrosion phenomenon, it is important to develop non-destructive techniques as well as predictive numerical modelling to assess the corrosion evolution of RC structures. This could help asset owners to adopt an efficient maintenance policy. The present study focuses on chloride-induced corrosion and the main issue of this paper is to design a specific test protocol to generate a "controlled" corrosion evolution versus time in order to bring some experimental evidences on the concrete cover cracking process due to corrosion and to determine relevant input parameters for the numerical modelling.

2 Experimental program

2.1 Materials and specimens

For the experimental campaign, twelve single-rebar specimens (500×125×100mm^3) were cast with a 600mm long and 20mm diameter steel rebar. This reinforcement bar was positioned to obtain a 30mm concrete cover at two sides of the specimen (Figure 1). The specimens designed with an asymmetric location of the rebar aim to get closer to reality. A Portland cement and siliceous aggregates were used for the concrete composition with a water to cement ratio of 0.73. This ratio is representative for former reinforced concrete structures. Moreover, it allows a faster penetration of the chloride ions during the accelerated corrosion test.

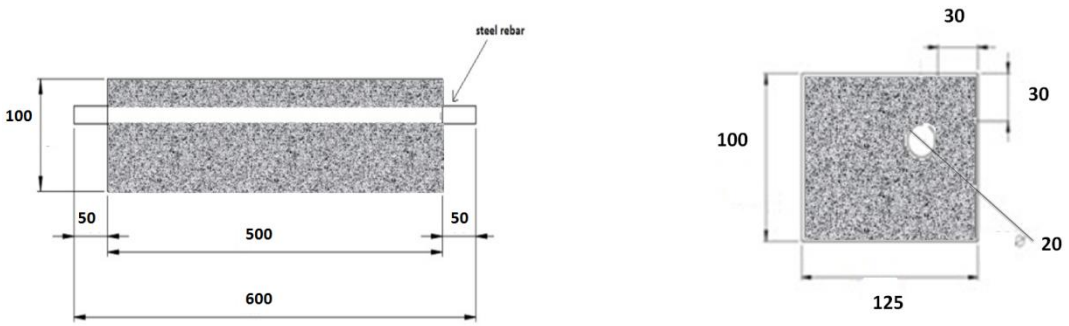

Figure 1. Schematic representation of RC specimens (dimensions in mm)

The cement type used for the concrete composition was CEM I 52.5 CP2 NF according to European standards. Concrete was prepared with aggregates having different particle size classes ((0/0.315 mm; 0.315/1 mm; 0.5/1 mm; 1/4 mm; 2/4 mm; 4/8 mm; 8/12 mm; 12.5/20 mm)). Compressive and tensile strengths were measured on concrete cylinders (160mm in diameter, 320mm in height) after 28 days according to NF EN 12390-3 [8] and NF EN 12390-6 [9] standards. The mean compressive strength is 32 MPa, the tensile strength is 2.6 MPa, the Young's modulus is 35 GPa and the Poisson's ratio is equal to 0.15.

2.2 Accelerated corrosion test and monitoring set-up

In this research, experimental investigations have been carried out in the laboratory under accelerated conditions. The set-up used for the accelerated corrosion test and the monitoring system are illustrated in Figure 2. Corrosion in the RC specimens was promoted by polarizing the embedded steel bars in the anodic direction using a power supply (Agilent 6614C, 100V, 0.5A) which delivered an imposed anodic current. The counter electrode (cathode) was an inert platinum titanium mesh (275mm long, 75mm wide) placed into a PVC tank containing an alkaline electrolyte (1g/L of NaOH, 4.65 g/L of KOH, 30 g/L of NaCl) which was glued on the top side of the concrete (in the middle of the specimen). All specimens were connected in series and a current density of 100 µA/cm² of steel was continually applied during the chosen exposure time (7, 14, 21, 28, and 35d). At the end of each considered exposure time, two specimens were disconnected from the electrochemical test set-up. One of these two specimens was used for the non-destructive electrochemical characterization and the other one was subjected to destructive measurements. The accelerated corrosion test was monitored using a data acquisition unit (Keysight 34970A): temperature of ambient air, supplied constant current, voltage per specimen, and total voltage were recorded every two hours.

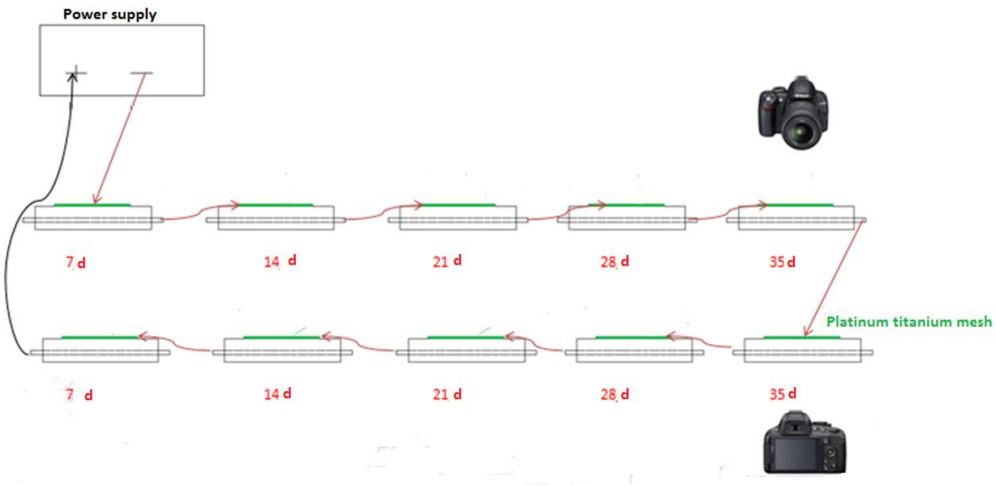

Figure 2. Scheme of the accelerated corrosion set-up

2.3 Electrochemical characterizations

Electrochemical characterizations of the rebar were performed after each exposure time of the accelerated test in order to determine the corrosion state. The imposed anodic current was interrupted during the measurements. Half-cell potential measurements (E_{corr}), linear polarization resistance measurements (LPR) and impedance spectroscopy (Re) were carried out using a potentiostat (Bio-Logic, PARSTAT 2263) and the usual electrochemical cell with three electrodes. The working electrode was the steel rebar, the reference electrode was a KCl saturated calomel electrode (SCE, 242 mV / SHE) and the counter electrode was a titanium platinum mesh. The same electrolyte as for the accelerated corrosion test was used.

Then the corrosion current density J_{corr} (µA/cm²) was calculated based on Eqn. (1):

$$J_{corr} = \frac{B}{R_p \ S} \quad (1)$$

with B a constant (26mV for corroding steel), R_p (ohm) the linear polarization resistance and S (cm²) the exposed steel surface (172.78 cm² in this study).

2.4 Experimental observations

Visual observations

At the end of the accelerated corrosion test, at first non-destructive observations were conducted. Special attention was given to the top and the front sides of specimens because of their lower concrete cover (30mm). Cracks widths were measured with a crack measuring magnifier (resolution 0.1mm) on these two surfaces. Then the specimens were sliced (125x100x20mm^3) for autopsy, considering corroded areas as illustrated in Figure 3. After 24h drying in an oven at 45°C, the slices were photographed and examined in order to characterize the crack pattern (angle and length) (Figure 4). The methodology developed by Sanz-Merino [10] was adopted (Figure 4-a) to determine the angular position. The length of the cracks in each cross-section was estimated by superimposing the photographs of the cross-section and a circle graduated every centimeter as shown in Figure 4-b. Then from both results an attempt was made to correlate what would be seen by the asset owner on the concrete surface in 2Dimensions and what happened inside the concrete with an aim of 3Dimensions.

Scanning Electron Microscopy observations

The slices were impregnated with an epoxy resin under vacuum (to prevent disbonding between concrete and steel when the corrosion damage was severe) and then cut into smaller samples which dimensions (2×4.5×4.5cm^3) fitted in the Scanning Electron Microscopy (SEM) observation room. The first objective is to

determine the corrosion product thickness and its length circling the perimeter of the rebar. The second objective is to observe the crack pattern and the transfer of the oxides through the cracks.

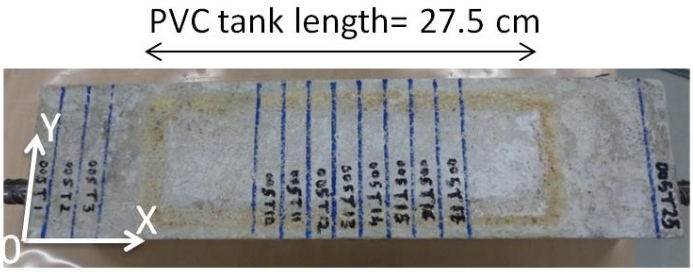

Figure 3. Graduated circles positioned on the two sides of a slice to measure (a) the crack angular position and (b) the crack length

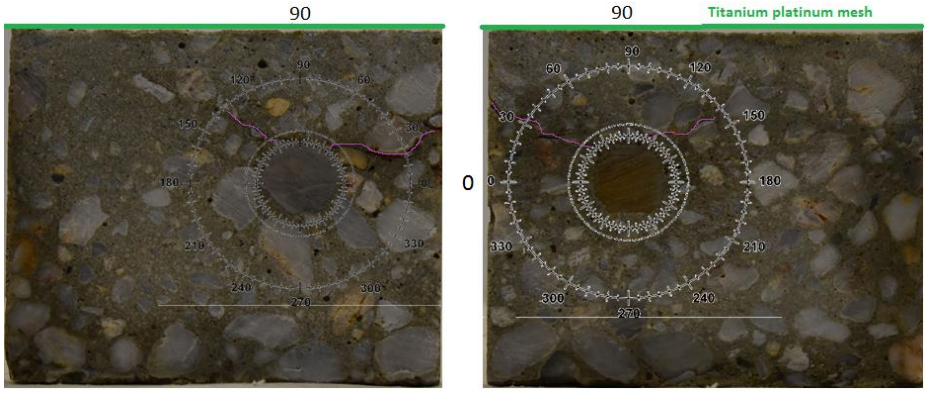

(a)

(b)

Figure 4. Determination of the crack angular position (a) and the crack length (b) after the accelerated corrosion test on the two sections of a slice

3 Experimental results

3.1 Voltage evolution during the accelerated corrosion test

During the accelerated corrosion test for each specimen the voltage was recorded. Figure 5 shows the time evolution of the voltage for the RC specimens. Before the test (time=0), the measured voltage reflects the electrical resistance of the specimens which are in a close range from 2.5 to 3 V except for the P004-7d specimen (3.3V). During the test, three consecutive stages can be distinguished. In the first stage, the observed voltage increase (about 1V) may be explained by the formation of resistive iron oxides (passive layer) [11], [12] around the rebar and also by the diffusion into the concrete and the filling up of the concrete pores by the oxides in the vicinity of the steel. In the second stage, the drastic voltage decrease (50% loss) can arise from the concrete cracking and the steel / concrete debonding. The last stage demonstrating a constant voltage (1.4V) appears for longer durations, 28d and 35d and is likely representative of a constant impedance of the corrosion layer. These preliminary observations need to be discussed considering the migration of the ionic species under galvanostatic control and particularly the penetration of the chloride ions. Analysis of these results is in progress.

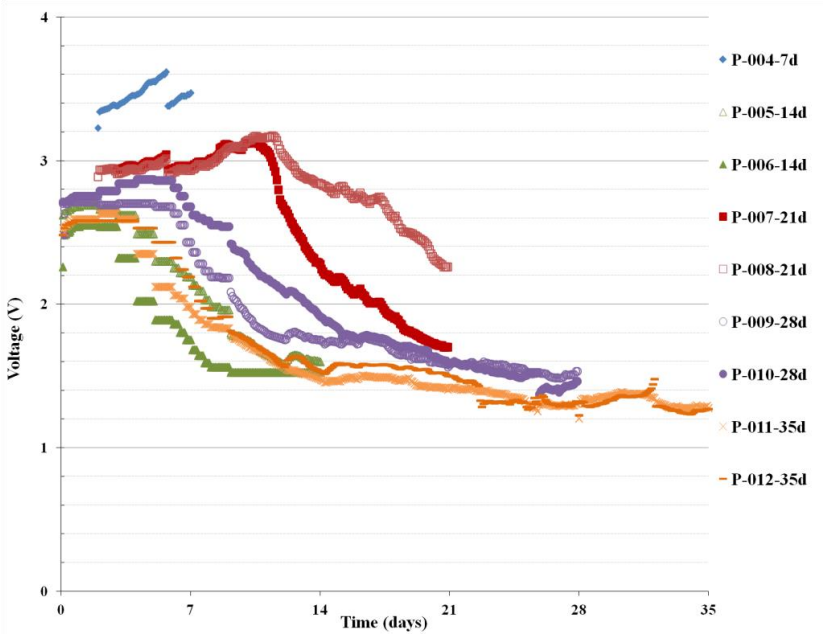

Figure 5. Voltage evolution during the accelerated corrosion test

3.2 Corrosion rate and crack patterns

Photos of all specimens were periodically taken to record the external changes (cracks and corrosion products) at the front side of specimen, while photographing the top side was only possible at the end of the corrosion process of the considered specimen. Figure 7 shows the corrosion signs and the cracks observed at the top side and the front side of two specimens after a 21 days accelerated corrosion test.

Regarding the top sides, specimen P-007 shows some stains of corrosion products and a visible crack roughly along the steel rebar whereas specimen P-008 is not damaged. However, regarding the front sides, the opposite behaviour is observed: specimen P-007 only exhibits a single spot of corrosion product while specimen P-008 shows significant corrosion products along the crack that follows the rebar. A possible explanation for this difference could be that the aggregate as well as the rebar's ribs are not homogeneously distributed and promote this heterogeneity.

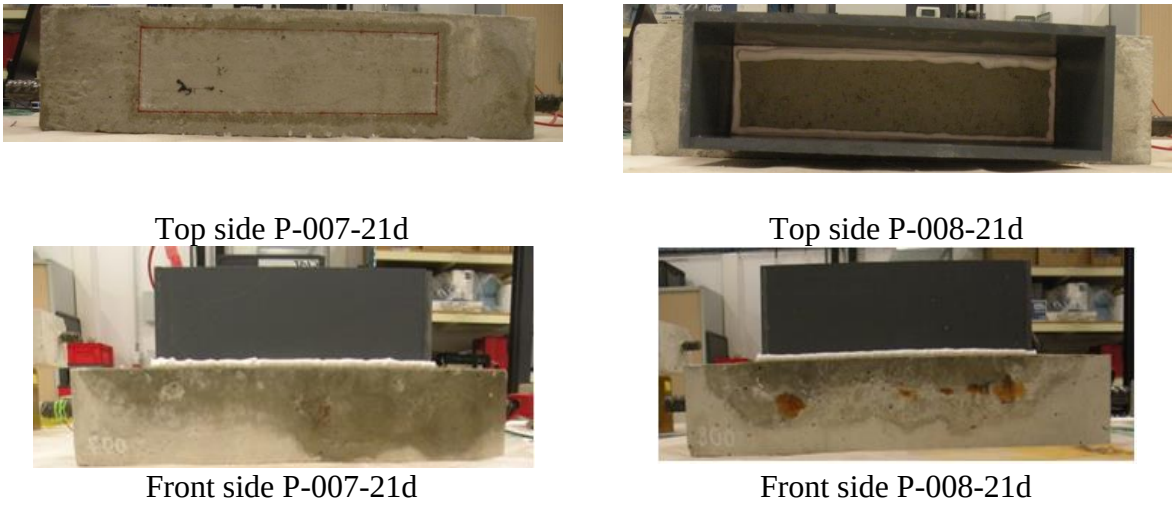

Figure 6. Qualitative results of the specimens after an accelerated corrosion of 21 days

Measured values of crack width (wider opening measured on top side and wider opening measured on front side) and of J_{corr} are presented in Figure 7. These results reveal that all corroded specimens for over 14 days have a J_{corr} equal to 10µA/cm² approximately except specimen P-004-7d corroded for 7 days. The proposed assumption is that at 7 days chloride ions have not reached the steel/concrete interface yet and consequently, the steel is still in a passive condition. Measurements of chloride ingress with $AgNO_3$ were made on each slice and the results obtained confirmed this assumption.

Regarding the crack width, the behaviour of corroded specimens appears to be different. As previously mentioned, all specimens are not cracked on the same side. As already suggested, this difference could be ascribed to the heterogeneity of the concrete (the random distribution of the aggregates into the cement paste). Besides, the crack on the top side is wider than the one on the front side. This observation might be attributed to the close localization of the counter electrode on the top side of the specimen (relative to the position of the steel rebar) that permits chloride ions to quickly reach the rebar (modification of the physico-chemical conditions that locally enhances the corrosion process).

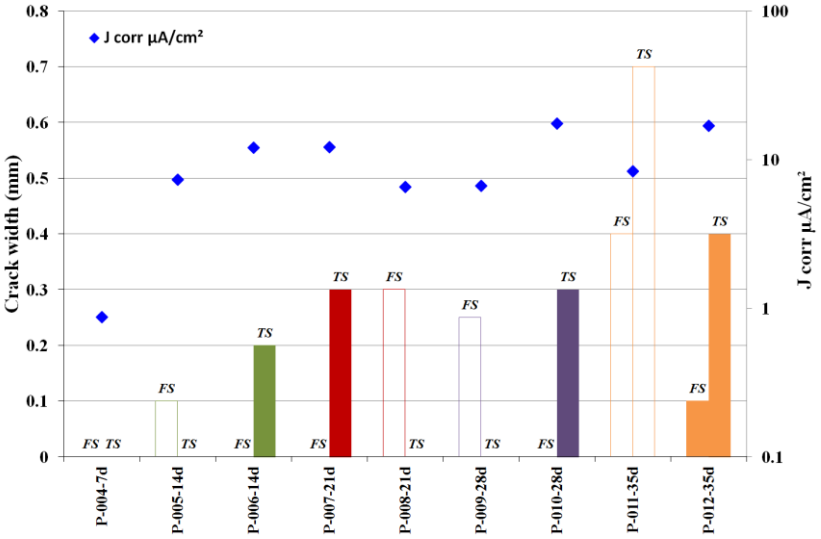

Figure 7. Crack width evolution and J_{corr} (FS:front side ; TS:top side)

Figure 8 shows the evaluation of the crack patterns (angular position (a), length (b) and width (c)) for each of the 16 sides of the eight slices of specimen P-008-21d. The cracks propagate from the steel/concrete interface to the concrete surface.

As shown in Figure 8-a, two groups of the position of the cracks near the steel surface are observed oriented close to 40° and 120° according to the graduated circle (see Figure 4-a). Two mains cracks seem to be displayed. Two sets of crack lengths could be identified, the first one is about 3cm long (crack extending through the entire concrete cover) and the second one is between 1 and 2cm long, see Figure 8-b. The lengths tend to fluctuate because of the distribution of the aggregates which influences the crack path. The graph in Figure 8-c corresponds to crack widths and shows the observed general trend. The crack widths are around 0.1 and 0.3mm.

The thickness of corrosion products is measured by Scanning Electron Microscopy at different zones along the steel/concrete interface (see Figure 9) and the perimeter represents the length of the shape of the rebar according to the volume of the corrosion products.

The minimum thickness of corrosion products varies from 50 to 57µm and the maximum thickness varies from 257 to 314µm (see Table 1). The highest thickness is located in the upper part of the steel rebar. This ‘expected’ difference could result from the distance between the counter electrode and the steel surface area. The closer they get, the more the corrosion process is forced. The crack width located on the top side is wider than the one located on the front side because the penetration path of the chloride ions to reach the steel surface area is the shortest.

Comparing the internal measurements ‘crack orientations’ and the widths measured on the sliced samples with the external observations (corrosion products spots on the front side of the specimens), the surface observations do not reflect the actual internal corrosion state at the steel/concrete interface.

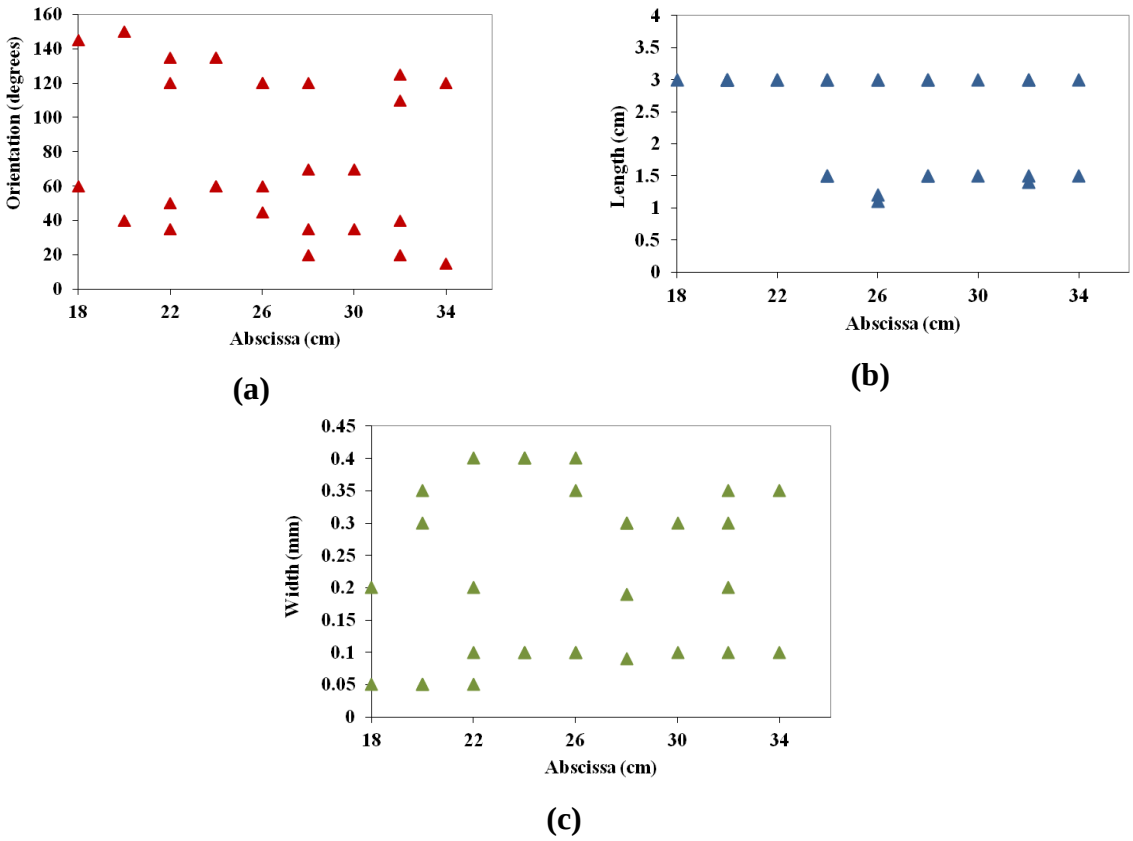

Figure 8. Measurement results for the characterization of the internal cracks a) angular position, b) length and c) width

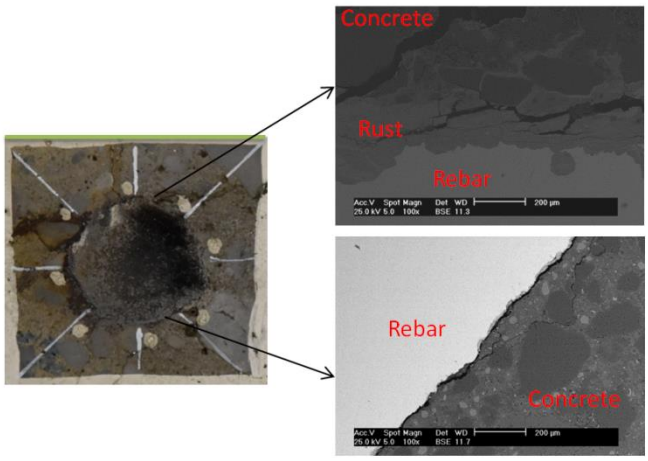

Figure 9. Methodology for the estimation of the rust layer thickness at different zones of the steel/concrete interface

Table I. Thickness of the corrosion products layers and corresponding visual distribution of evidences on the front side

Slices	Maximum thickness of the corrosion products layers (µm)	Minimum thickness of the corrosion products layers (µm)	Perimeter of the corrosion products layers Max/Min (µm)
P-008-21d-T10	257	57	2 617 / 5 233
P-008-21d-T13	314	63	5 233 / 5 233
P-008-21d-T16	257	50	5 233 / 10 467
Mean values	276	56.6	

4 Conclusions

Cracks due to corrosion of the steel reinforcement in concrete specimens have been investigated using an accelerated corrosion test. A specific methodology able to describe the main features of the tests is proposed. Based on the results, the following preliminary conclusions can be drawn:

- Three consecutive stages in the corrosion process can be distinguished: the increase of the polarization resistance may be explained by the development of resistive iron oxides (passivation layer). The second stage could highlight the loss of the resistance of the set due to the concrete cracking and the loss of bond between the steel and concrete surface area, respectively. Regarding the third stage, the observed effect may be attributed to the fact that the properties of corrosion layers remain unchanged. Then, the

value of the voltage at the end of the test certainly reflects the resistance of both cracked concrete cover and iron oxide layer.

- After 7 days, an active state of corrosion is not clearly observed and this could be explained by the fact that a sufficient amount of chlorides to initiate corrosion has not reached the steel/concrete interface.
- After 21 days, the two cracks orientations (40°/120°), lengths (3 cm/1.6 cm) and width (0.3 mm/ 0.1 mm) are coherent for the same specimen.
- From Scanning Electron Microscopy results, corrosion products thicknesses are in the range of 56.6 µm/ 276 µm.
- The corrosion-product spots on the surface of the concrete specimens do not reflect the internal corrosion state at the steel/concrete interface of the specimen.

Results reported here have to be confirmed after achieving the measurements on all specimens. In the following steps, some of the experimental results such as the thickness and the display of the oxide layer will be used as input data for the numerical modelling of corrosion-induced cracks. The other experimental results associated with the crack patterns will allow a comparison between the experience and the modelling. An experimental test is in progress to characterize mechanical properties of these products to improve the modelling of the corrosion product layer in the numerical simulation.

5 References

1. Cairns, J. and Millard, S. (1999). In: Reinforcement corrosion and its effect on residual strength of concrete structures, Proceedings of the 8 th International Conference Structural Faults+Repair-99, London.
2. Weyers, R. and Prowell, B. (1996). Corrosion inhibiting repair and rehabilitation treatment process for reinforced concrete structures. Cement and Concrete Composites, p. 459.
3. Mehta, P.K. and Monteiro, P.J.M. (1997). In Concrete: structures, Properties and Materials., Indian Concrete institute: India.
4. Richard, B. and Quiertant, M. (2012). Influence of accelerated corrosion on the reinforced cover concrete cracking behavior: experimental and numerical study. European Journal of Environmental and Civil Engineering, vol 16(3-4), pp 450-459.
5. Richard, B. and Quiertant, M. (2016). Experimental and numerical analysis of corrosion-induced cover cracking in reinforced concrete sample. Computers and Concrete, vol 18(3): pp 421-439.
6. Jamali, A. (2013), Modeling of corrosion-induced concrete cover cracking: A critical analysis. Construction and Building Materials, vol. 42, pp. 225-237.
7. Dehoux, A. (2012) Propriétés mécaniques des couches de produits de corrosion à l'interface acier / béton., Université Pierre et Marie Curie.
8. N.E. (2001). Testing hardened concrete. Part 6: Tensile splitting strength of test specimens.
9. NF EN 12390-3., (2003).Testing hardened concrete. Part 3: Compressive strength of test specimens
10. Sanz Merino, B. (2014). Experimental and numerical study of cracking of concrete due to corrosion., Universidad Politecnica de Madrid Escuela Tecnica Superior de Ingeniros de Caminos, Canales y Puertos. p. 254.
11. Caré, S. and Raharinaivo, A. (2007) Influence of impressed current on the initiation of damage in reinforced mortar due to corrosion of embedded steel, vol. 37: pp. 1598-1612.
12. Poupard, O. (2004) Corrosion by chlorides in reinforced concrete: Determination of chloride concentration threshold by impedance spectroscopy. Cement and Concrete Research,vol. 34: pp. 991-1000.